NANO LETTERS

2008
Vol. 8, No. 2
606−610

Reversible Polarization Control of Single Photon Emission

Robert J. Moerland*

Optical Sciences Group, Faculty of Science and Technology and MESA+ Institute for Nanotechnology, University of Twente, P.O. Box 217, NL-7500AE, Enschede, The Netherlands

Tim H. Taminiau

ICFO-Institut de Ciencies Fotoniques, Mediterranean Technology Park, 08860 Castelldefels (Barcelona), Spain

Lukas Novotny

The Institute of Optics, University of Rochester, Rochester New York 14627

Niek F. van Hulst

ICFO - Institut de Ciencies Fotoniques, Mediterranean Technology Park, 08860 Castelldefels (Barcelona), Spain, and ICREA - Institució Catalana de Recerca i Estudis Avançats, 08015 Barcelona, Spain

Laurens Kuipers†

FOM Institute for Atomic and Molecular Physics (AMOLF) Kruislaan 407, NL-1098SJ, Amsterdam, The Netherlands

Received November 20, 2007; Revised Manuscript Received December 17, 2007

ABSTRACT

We present reversible and a-priori control of the polarization of a photon emitted by a single molecule by introducing a nanoscale metal object in its near field. It is experimentally shown that, with the metal close to the emitter, the polarization ratio of the emission can be varied by a factor of 2. The tunability of polarization decays, when the metal is displaced by typically 30 nm. Calculations based on the multiple multipole method agree well with our experiments and predict even further enhancement with a suitable nanoantenna design.

Spontaneous emission of single quantum systems, such as organic molecules and quantum dots, is finding widespread application in sensing and nanoscale imaging of (bio)-chemical systems.[1,2] The well-defined photon statistics is explored for quantum information applications.[3,4] Control over the photodynamics and polarization of single emitters would provide photons on demand with a chosen polarization. Indeed, manipulation of radiative decay is being studied by placing (single) emitters in photonic crystals,[5] dielectric nanospheres,[6,7] and near (nanoscale) metal structures.[8−12] It is well known that breaking symmetry with finite-sized nano-objects leads to deviations of spontaneous emission properties of the emitter such as changes in lifetime[13−15] and radiation pattern.[16,17] With various near-field scanning probe methods, employing, for example, aperture probes and metallic nanospheres, different groups have observed the dependence of fluorescence lifetime on both the horizontal and vertical probe−molecule distance.[18,19,10,11] Furthermore, together with quantum dots and nitrogen-vacancy centers in diamond, single molecules are good candidates to be used as single-photon sources.[4] By structuring the molecule's surroundings, for example, with a photonic crystal or microcavity, the photons will be emitted into the mode dictated by the local environment.[5,20] However, dynamic and reversible control of the polarization of the emission on a per-photon base has proven to be difficult, because this involves dynamically and controllably changing the molecule's nanoenvironment. Therefore, usually once a mode has been set for the molecule to emit into, it cannot be changed. In this letter, we show a-priori control and reversible change of the polarization of

* Corresponding author. E-mail: r.moerland@utwente.nl.
† E-mail address: l.kuipers@amolf.nl.

10.1021/nl073026y CCC: $40.75
Published on Web 01/15/2008

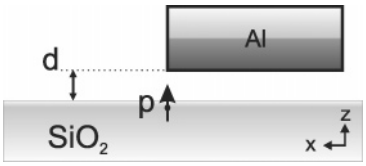

Figure 1. Principle of polarization control on the single emitter level. An embedded molecule (represented by a dipole **p**) interacts with the edge of a metal object (aluminum disk). The polarization of emitted photons can be controlled by the relative separation between the molecule and the edge. The disk ($\epsilon = -38.4 + 10.2i$) is 110 nm in diameter and has a thickness of 40 nm. The separation between the disk and the surface d is 20 nm and the molecule is 1 nm below the surface.

the emitted light of a single molecule by manipulating the local environment of the molecule with a nanoscale object. Verified by experimental results, we present a theoretical three-dimensional model system that quantifies our proposed method.

The method is depicted schematically in Figure 1. An emitter, for example, a molecule, is embedded at 1 nm depth in a transparent substrate ($\epsilon = 2.5$) with a transition dipole perpendicular to the substrate−air interface. The emitter is placed near a nanoscale metal object, in this case an aluminum disk ($\epsilon = -38.4 + 10.2i$) of 110 nm diameter and 40 nm height, to modify the environment of the radiating dipole. The disk is placed at a height of $d = 20$ nm above the surface. Figure 1 depicts the particular configuration when the dipole is located right underneath the vertical edge of the disk. We calculate the local electric field distribution by use of the multiple multipole (MMP) method.[16] In the calculation, the radiation is "collected" with a high-NA objective positioned in the $-z$ half-space with its optical axis aligned to the z-axis. For this situation, we calculate the x-polarized and y-polarized intensity distributions in the back focal plane of the objective. For a z-oriented dipole, having no objects in its near field, one expects an emission pattern that has a cylindrical symmetry.[21] Consequently, the polarization of the emission in the back focal plane of the objective is equally partitioned in x-polarized and y-polarized radiation (i.e., radial polarization). If the nanoscale aluminum disk is introduced into the near field, it can control both the emission pattern and the polarization. The results for a configuration such as shown in Figure 1 are depicted in Figure 2a,b. We find that the metal disk's edge influences the dipole's emission, inducing an in-plane (i.e., horizontal) component perpendicular to the vertical edge of the disk. This effectively increases the polarization component perpendicular to the metal edge (Figure 2a). At the same time, polarization components parallel to the vertical metal edge are suppressed (Figure 2b). The influence on the polarization is maximal for a z-oriented dipole, because an in-plane orientation of the dipole will bias the polarization of the radiation in a certain direction that makes the relative change of the polarization direction smaller.

For our experiments, we use a home-built near-field scanning optical microscope (see Figure 3). Light from an argon−krypton laser ($\lambda = 514$ nm, Ar^+ line) is coupled into a focused ion beam-modified near-field fiber probe coated

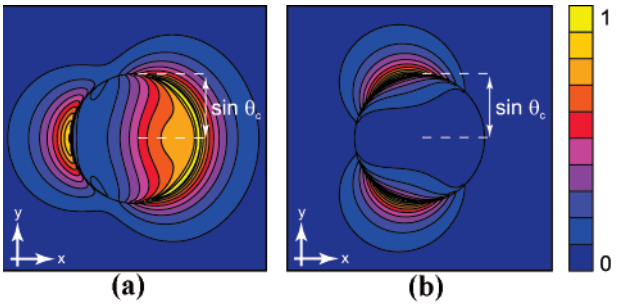

Figure 2. Calculated radiation patterns of a single molecule located underneath the edge of an aluminum disk (see Figure 1). The patterns correspond to the polarized intensity distributions in the back focal plane of the collection objective. The circles in both images indicate the critical angle of total internal reflection: $\theta_c = 41°$. The molecule has its emission dipole in the z-direction. (a) Polarization in x-direction. (b) Polarization in y-direction. The metal object influences the dipole's emission, inducing an in-plane component perpendicular to the nearest vertical edge of the disk. This causes an increase of the polarization component perpendicular to the edge (arbitrary units, linear scaling, same scale in both figures).

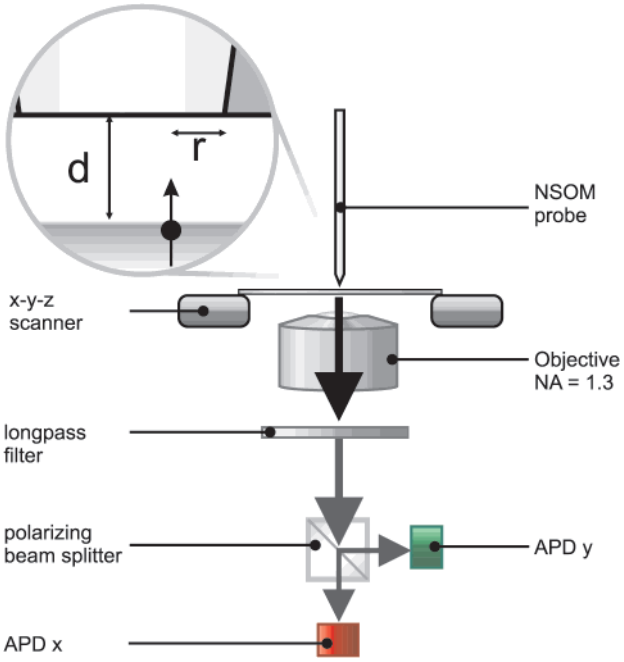

Figure 3. Schematic depiction of the experimental setup. Light from an Ar−Kr laser (not shown) is coupled into the near-field probe. Fluorescence, emitted by single molecules in the sample, is collected by an objective (NA 1.3) and separated from the laser light by a long pass filter. A polarizing beam splitter divides the radiation into its two orthogonal polarization components that are detected with APD x and APD y, respectively. The inset shows a schematic cross-section of an aperture probe nearby a z-oriented molecule. The sharp glass−metal edge is used to control the polarization of the emission of the molecule.

with aluminum.[22] This probe is used to both excite molecules in the sample and control the polarization of their emission. As such, the role of the disk edge in Figure 1 is performed by the sharp metal−glass transition at the edge of the aperture. The distance between the sample and the probe is controlled using shear-force feedback. When engaged, the shear-force feedback results in a probe−substrate distance

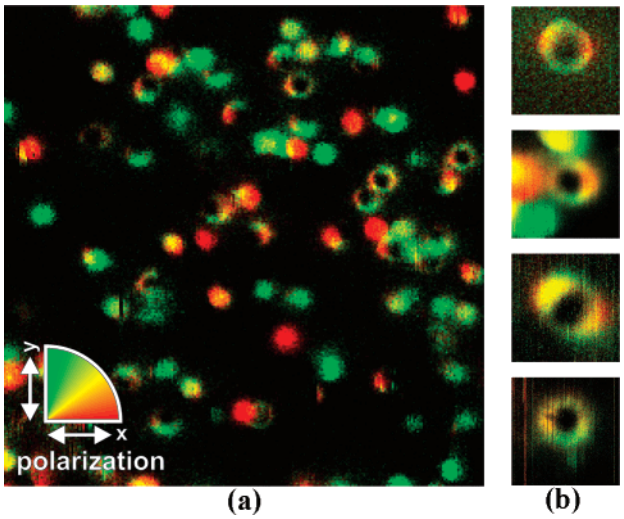

Figure 4. (a) Single molecule polarization map obtained by raster scanning the near-field probe over the surface of the sample. Rings, the result of the interaction of the *z*-oriented field from the probe with *z*-oriented molecules, can clearly be distinguished from the in-plane oriented molecules, which are represented by the colored spots. The polarization is color coded: x = red, and y = green (see inset). Excitation wavelength: 514 nm. Scan area: $3 \times 3\ \mu$m. (b) Close-up of four different *z*-oriented molecules measured with different probes. The change in color of the ring around the perimeter reflects the clear change in the degree of polarization of the emission radiated by the molecule, as a function of probe position. Scan area: 500×500 nm.

of 10−25 nm.[23] With a piezo *x*-*y*-*z* driver, we control the position of the molecule relative to the metal rim. The light emitted by the molecule is collected using a 1.3 NA oil-immersion objective. A long-pass filter blocks the excitation light coming from the probe. Finally, we probe the projected polarization state[24,25] of the single emitter emission using a polarizing beam-splitter. The *x*- and *y*-polarized radiation is independently measured using avalanche photodiodes (APD *x* and APD *y*, respectively).

Samples are prepared by dissolving 0.5% poly(methylmethacrylate) in toluene and adding carbocyanine ($DiIC_{18}$, $\lambda_{em,peak} = 570$ nm) dye molecules to a 10^{-8} molar concentration. This solution is spin-coated on plasma-etched glass substrates, resulting in a thin polymer matrix containing embedded $DiIC_{18}$ molecules. The samples are dried in air at room temperature. This procedure results in a polymer matrix with dispersed single molecules, fixed in position and orientation on the time scale of the experiment.[17]

The molecules are excited by the near field at the aperture of the probe, using circularly polarized incident light. By raster scanning the probe over the sample, the amount of photons detected by each APD as a function of probe position is obtained. The scan yields an image map containing the locations of each molecule and the projected polarization state of the emitted light at each position of the probe. A typical image is shown in Figure 4. Here, the following color-coding method is used: the signal from APD *x* is displayed in red, and the signal from APD *y* is displayed in green. Clearly visible beside all the in-plane oriented molecules, which show up as color-filled spots, are ring-shaped patterns. These excitation patterns are the result of fluorescence of *z*-oriented molecules that are only excited by an electric field component in the *z*-direction, which is only found at the rim of the aperture.[26−29] A close-up of four individual molecules, each from a different sample and measured with different probes, is shown in Figure 4b. These close-ups show that the degree of polarization is reversibly altered while scanning the probe over the molecule, as is evident from the change of color around the perimeter of the ring-shaped pattern.

The experimental results therefore prove that the polarization of the emitted photons can be reversibly influenced with a metal nanostructure in close proximity. Under the assumption of perfect axial symmetry of the aperture, the intensity of the measured *x*-polarized radiation I_x can be written as

$$I_x(r,d,\phi) = A(r,d)\cos^2(\phi) + B(r,d)\sin^2(\phi) \qquad (1)$$

where r is the in-plane metal edge−molecule separation, d is the probe−surface separation, ϕ is the azimuthal angle and $A(r,d)$ and $B(r,d)$ are functions that contain the excitation efficiency and the radiative properties of the molecule. For the *y*-polarized radiation, $A(r,d)$ and $B(r,d)$ are interchanged. Thus, an induced polarization anisotropy, that is, $I_x \neq I_y$, at a given azimuthal angle ϕ will result in a periodic modulation of the anisotropy as a function of ϕ.

The polarization ratio of the fluorescence is defined as I_x/I_y, where I_x and I_y are the number of photons measured by APD *x* and APD *y*, respectively. We can quantify the measured polarization ratio as a function of angle for a single molecule; typical examples for three molecules are shown in Figure 5. A clear periodic modulation of the polarization ratio with ϕ is visible. Thus, the polarization ratio of the photon emission indeed changes in a controlled and reversible manner as the molecule's relative position moves around the perimeter of the probe. As shown in Figure 5, it should be noted that from molecule to molecule differences can be observed both in the magnitude and the symmetry of the periodic behavior. We attribute this diversity to subtle differences both in the orientation of each molecule with respect to the sample surface and the exact distance between molecule and metal edge. We have analyzed these effects more quantitatively for molecule 1 in Figure 5. The measured polarization ratio for molecule 1 goes up to a factor of slightly more than 2 for $\phi = 0$. The measurements can be reproduced by correcting for a slight tilt of the probe with respect to the sample surface and a light bias toward the *x*-polarization due to a small tilt of molecule 1. We use the calculated dependence of the polarization ratio on the disk−sample distance d in the model in Figure 1 to describe the effect of probe tilt: for each position of the probe, that is, angle ϕ in Figure 5, the experimentally obtained polarization ratio gives from the calculation a distance of the disk to the surface that has the same polarization ratio as a result. As ϕ increases, the edge of the disk is forced to describe a (tilted) circle in space to model the ring-shaped metal−glass edge of the end face of the probe. Additionally, a small tilt of the molecule's dipole may result in a bias toward a certain polarization state of the emission. Consequently, a fit of a tilt angle for the probe of 9° plus a bias of 16% of the total

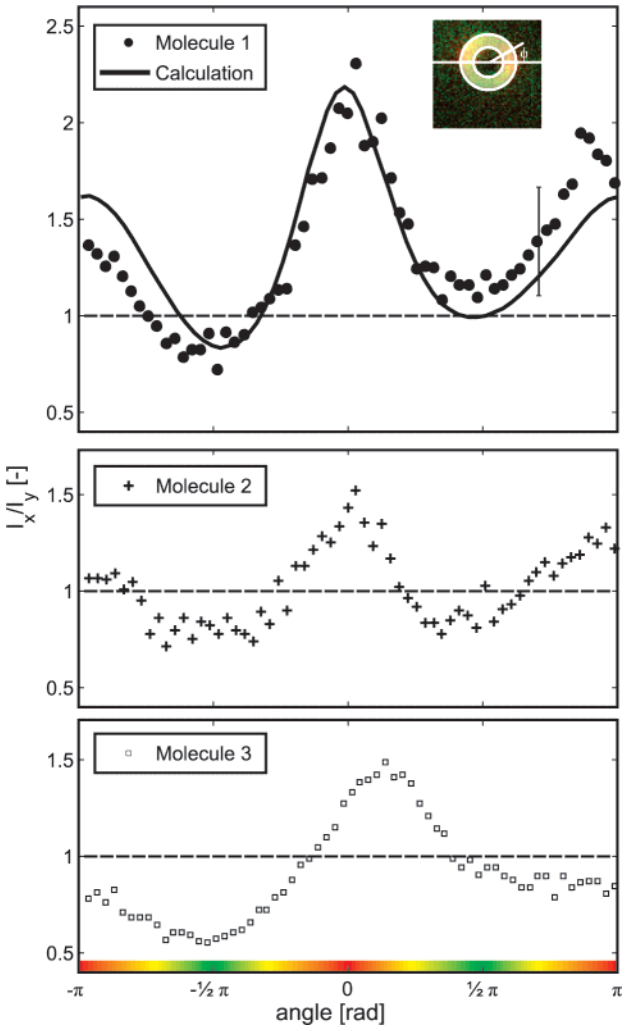

Figure 5. Polarization ratio I_x/I_y as a function of the angle ϕ for *z*-oriented molecules. The inset shows an image of a typical obtained molecule map. Data from the area between the white circles are integrated radially and plotted as individual data points ($\Delta\phi = 0.032\pi$). The boundaries of integration are positioned such that they define the points in space where the single molecule fluorescence signal is just distinguishable from the background signal. A typical error bar, shown for one data point, shows the maximum standard deviation that occurred over all angles ϕ. Other error bars are left out for clarity. As the relative position of the metal probe changes, the polarization ratio of the emitted photons changes and a clear periodic modulation of the polarization ratio with ϕ can be seen. The calculation shows that if a small probe tilt and a small polarization bias due to an inclination of the molecule's dipole are taken into account, a good correspondence is obtained between model and experiment (solid curve).

collected power toward the *x*-polarization due to tilt of the molecule yields a good correspondence between experiment and calculation (solid curve in Figure 5, molecule 1). According to the approximation of a tilted probe, the probe is then closest to the surface at an azimuthal angle of $\phi = 0.18\pi$ with a distance of 21 nm between the glass−metal edge and the surface. Possibly, a bias might also be induced by other causes, such as the tilt of the probe itself. These effects need further investigation. Here, for simplicity all effects of bias are included in the tilt of the molecule. Molecules 2 and 3 show less asymmetric oscillations and

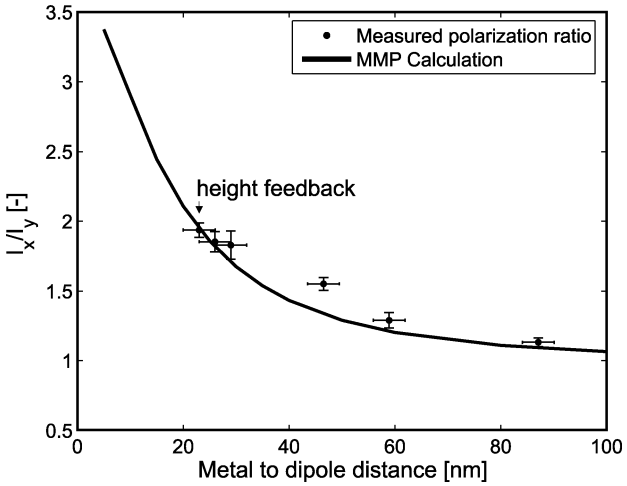

Figure 6. Polarization ratio as a function of distance. The measured polarization ratio goes up to a factor of 2 for the engaged height feedback. The rapid drop within 30−40 nm to values near unity, which is the limit value for an unperturbed molecule, reveals that the molecule is influenced only in the near field.

are likely to be less tilted away from the *z*-orientation. Finally, minor asymmetry in the position of the maxima is attributed to small imperfections in the circular aperture edge of the probe.

In our experiments, we have obtained from molecule 1 and with the same probe the degree of polarization control as a function of gap width, that is, the height of the probe above the molecule. To enhance signal-to-noise, the polarization ratio is determined by integrating I_x/I_y from $\phi = -0.13\pi$ to $\phi = 0.13\pi$ (cf. Figure 5). The values obtained are plotted in the graph shown in Figure 6. The absolute height, corresponding to an engaged shear-force feedback, is set to 23 nm as found at $\phi = 0$ for the model incorporating probe tilt. The following points can be observed: the measured ratio I_x/I_y for small distances, for example, for the engaged feedback probe−surface distance, is approximately 2. Furthermore, the fact that the polarization ratio rapidly decays when the separation between the probe and the molecule is increased by only 30−40 nm reveals that the influence of the metal is a true near-field effect. Finally, for probe−molecule distances that are "far" away the polarization ratio approaches unity, which is expected for a *z*-oriented single dipole in stratified media without any objects in its near field. A full three-dimensional MMP calculation, shown in Figure 6 as a black curve, confirms the observed behavior. Additionally, this calculation indicates that even better control can readily be obtained by further decreasing the distance between the emitter and the metal. We note that although in the experiment a ringlike structure (the probe) was used instead of a metal disk, the experiments and calculations match quite well. Because the aperture of the probe used in this experiment is 130 nm in diameter, we believe that this is due to the fact that the influence of the metal edge that is not right above the molecule is negligible .

In summary, we have shown in experiment and by calculation that the polarization of single photon emission can be changed and reversibly controlled on the nanoscale.

The control is achieved by placing a metal nanosized object in the form of the sharp glass−metal edge of an aperture-type probe into the near field of a single molecule. Experimentally, a polarization anisotropy of a factor of up to 2 is induced. The rapid decay of the polarization anisotropy to nearly unity, that is, within a few tens of nanometers distance, shows that the control is strongly dependent on the interaction of the near field of the dipole with the metal probe. Both experiments and calculations for the given control scheme show that the degree of polarization is altered in favor of the polarization component parallel to the dielectric interface and perpendicular to the closest vertical metal edge of the aluminum probe. Our calculations predict that a factor of 3 of polarization anisotropy should well be possible by placing the metal objects closer to the emitter. An even stronger emission control is expected for resonant structures that exhibit enhanced localized fields and are in resonance with the molecule.[30]

Acknowledgment. This work is part of the research program of the Stichting voor Fundamenteel Onderzoek der Materie (FOM), which is financially supported by the Nederlandse Organisatie voor Wetenschappelijk Onderzoek (NWO) and by the U.S. Department of Energy (Grant DE-FG02-01ER15204).

References

(1) Lill, Y.; Martinez, K. L.; Lill, M. A.; Meyer, B. H.; Vogel, H.; Hecht, B. Kinetics of the initial steps of G protein-coupled receptor-mediated cellular signaling revealed by single-molecule imaging. *ChemPhysChem* **2005**, *6* (8), 1633−1640.

(2) Friedrich, A.; Hoheisel, J. D.; Marme, N.; Knemeyer, J. P. Dna-probes for the highly sensitive identification of single nucleotide polymorphism using single-molecule spectroscopy. *FEBS Lett.* **2007**, *581* (8), 1644−1648.

(3) Moerner, W. E. Single-photon sources based on single molecules in solids. *New J. Phys.* **2004**, *6*, 88.

(4) Brunel, C.; Lounis, B.; Tamarat, P.; Orrit, M. Triggered source of single photons based on controlled single molecule fluorescence. *Phys. Rev. Lett.* **1999**, *83* (14), 2722−2725.

(5) Lodahl, P.; van Driel, A. F.; Nikolaev, I. S.; Irman, A.; Overgaag, K.; Vanmaekelbergh, D. L.; Vos, W. L. Controlling the dynamics of spontaneous emission from quantum dots by photonic crystals. *Nature* **2004**, *430*, 654−657.

(6) Barnes, M. D.; Kung, C. Y.; Whitten, W. B.; Ramsey, J. M.; Arnold, S.; Holler, S. Fluorescence of oriented molecules in a microcavity. *Phys. Rev. Lett.* **1996**, *76*, 3931−3934.

(7) Schniepp, H.; Sandoghdar, V. Spontaneous emission of europium ions embedded in dielectric nanospheres. *Phys. Rev. Lett.* **2002**, *89* (25), 257403.

(8) Drexhage, K. H. *Prog. Opt.* **1974**, *12*, 163.

(9) Steiner, M.; Schleifenbaum, F.; Stupperich, C.; Failla, A. V.; Hartschuh, A.; Meixner, A. J. Microcavity-controlled single-molecule fluorescence. *ChemPhysChem* **2005**, *6* (10), 2190−2196.

(10) Kuhn, S.; Hakanson, U.; Rogobete, L.; Sandoghdar, V. Enhancement of single-molecule fluorescence using a gold nanoparticle as an optical nanoantenna. *Phys. Rev. Lett.* **2006**, *97* (1), 017402.

(11) Anger, P.; Bharadwaj, P.; Novotny, L. Enhancement and quenching of single-molecule fluorescence. *Phys. Rev. Lett.* **2006**, *96* (11), 113002.

(12) Tam, F.; Goodrich, G. P.; Johnson, B. R.; Halas, N. J. Plasmonic enhancement of molecular fluorescence. *Nano Lett.* **2007**, *7* (2), 496−501.

(13) Ambrose, W. P.; Goodwin, P. M.; Martin, J. C.; Keller, R. A. Alterations of single-molecule fluorescence lifetimes in near-field optical microscopy. *Science* **1994**, *265*, 364−367.

(14) Bian, R. X.; Dunn, R. C.; Xie, X. S.; Leung, P. T. Single molecule emission characteristics in near-field microscopy. *Phys. Rev. Lett.* **1995**, *75* (26), 4772−4775.

(15) Girard, C.; Martin, O. J. F.; Dereux, A. Molecular lifetime changes induced by nanometer scale optical fields. *Phys. Rev. Lett.* **1995**, *75* (17), 3098−3101.

(16) Novotny, L. Single molecule fluorescence in inhomogeneous environments. *Appl. Phys. Lett.* **1996**, *69*, 3806−3808.

(17) Gersen, H.; Garcia-Parajo, M. F.; Novotny, L.; Veerman, J. A.; Kuipers, L.; van Hulst, N. F. Influencing the angular emission of a single molecule. *Phys. Rev. Lett.* **2000**, *85*, 5312−5315.

(18) Xie, X. S.; Dunn, R. C. Probing single-molecule dynamics. *Science* **1994**, *265*, 361−364.

(19) Trautman, J. K.; Macklin, J. J. Time-resolved spectroscopy of single molecules using near-field and far-field optics. *Chem. Phys.* **1996**, *205*, 221−229.

(20) Moreau, E.; Robert, I.; Gerard, J. M.; Abram, I.; Manin, L.; Thierry-Mieg, V. Single-mode solid-state single photon source based on isolated quantum dots in pillar microcavities. *Appl. Phys. Lett.* **2001**, *79* (18), 2865−2867.

(21) Ford, G. W.; Weber, W. H. Electromagnetic interactions of molecules with metal surfaces. *Phys. Rep.* **1984**, *113* (4), 195−287.

(22) Veerman, J. A.; Otter, A. M.; Kuipers, L.; van Hulst, N. F. High definition aperture probes for near-field optical microscopy fabricated by focused ion beam milling. *Appl. Phys. Lett.* **1998**, *72*, 3115−3117.

(23) Karrai, K.; Grober, R. D. Piezoelectric tip-sample distance control for near-field optical microscopes. *Appl. Phys. Lett.* **1995**, *66*, 1842−1844.

(24) Lee, K. G.; Kihm, H. W.; Kihm, J. E.; Choi, W. J.; Kim, H.; Ropers, C.; Park, D. J.; Yoon, Y. C.; Choi, S. B.; Woo, H.; Kim, J.; Lee, B.; Park, Q. H.; Lienau, C.; Kim, D. S. Vector field microscopic imaging of light. *Nat. Photonics* **2007**, *1* (1), 53−56.

(25) Gersen, H.; Novotny, L.; Kuipers, L.; van Hulst, N. F. On the concept of imaging nanoscale vector fields. *Nat. Photonics* **2007**, *1* (5), 242−242.

(26) Betzig, E.; Chichester, R. J. Single molecules observed by near-field scanning optical microscopy. *Science* **1993**, *262*, 1422−1425.

(27) Veerman, J. A.; Garcia-Parajo, M. F.; Kuipers, L.; van Hulst, N. F. Single molecule mapping of the optical field distribution of probes for near-field microscopy. *J. Microsc. Oxford* **1999**, *194*, 477−482.

(28) Sick, B.; Hecht, B.; Wild, U. P.; Novotny, L. Probing confined fields with single molecules and vice versa. *J. Microsc. Oxford* **2001**, *202*, 365−373.

(29) Moerland, R. J.; van Hulst, N. F.; Gersen, H.; Kuipers, L. Probing the negative permittivity perfect lens at optical frequencies using near-field optics and single molecule detection. *Opt. Express* **2005**, *13* (5), 1604−1614.

(30) Taminiau, T. H.; Moerland, R. J.; Segerink, F. B.; Kuipers, L.; van Hulst, N. F. $\lambda/4$ resonance of an optical monopole antenna probed by single molecule fluorescence. *Nano Lett.* **2007**, *7* (1), 28−33.

NL073026Y